frontiers | Frontiers in Materials

TYPE Original Research
PUBLISHED 15 July 2025
DOI 10.3389/fmats.2025.1602341



OPEN ACCESS

EDITED BY
Nicholas Thom,
University of Nottingham, United Kingdom

REVIEWED BY
Mahmoud Ebrahimi,
University of Maragheh, Iran
Guojian Liu,
Suzhou University of Science and Technology, China

*CORRESPONDENCE
Lei Wang,
leo@mails.cqjtu.edu.cn

RECEIVED 29 March 2025
ACCEPTED 01 July 2025
PUBLISHED 15 July 2025

CITATION
Yan Y, Li W and Wang L (2025) Effect of recycled aggregate and freeze-thaw cycles on fatigue performance of asphalt concrete. *Front. Mater.* 12:1602341.
doi: 10.3389/fmats.2025.1602341



# Effect of recycled aggregate and freeze-thaw cycles on fatigue performance of asphalt concrete

Yihong Yan[1], Wenbo Li[1] and Lei Wang[2]*

[1]School of Transportation, Changsha University of Science and Technology, Changsha, China,
[2]College of Traffic and Transportation, Chongqing Jiaotong University, Chongqing, China

Fatigue damage is a primary mode of failure in asphalt pavements under repeated traffic loading. The incorporation of recycled concrete aggregate (RCA) in asphalt mixtures addresses issues of construction waste landfilling while enhancing sustainability. This study investigated the influence of RCA sizes and freeze-thaw (F-T) cycles on fatigue lives of recycled aggregate asphalt concrete (RAAC) through laboratory tests. Three RCA size fractions (4.75–9.5 mm, 9.5–13.2 mm, and 13.2–16 mm) underwent Los Angeles abrasion tests to quantify morphological changes, including convexity, axiality coefficient (AC), and roundness. After 800 abrasion rotations, fine RCA showed minimal convexity reduction of approximately 0.4%, whereas coarse RCA exhibited a greater reduction exceeding 1.0%. Semi-circular bend (SCB) fatigue tests revealed that RAAC specimens with finer RCA consistently exhibited better fatigue resistance and higher stiffness modulus retention compared to medium and coarse gradations. Grey correlation analysis indicated a strong correlation between RCA size and fatigue life, with AC identified as the most influential morphological index. Fatigue life predictions using Basquin model demonstrated high accuracy ($R^2$ > 0.90). Furthermore, F-T cycles accelerated damage accumulation and stiffness reduction in RAAC over fatigue loading repetitions. These findings underscore the critical role of RCA particle morphology in enhancing RAAC durability under coupled environmental and mechanical loading conditions.

KEYWORDS

**recycled concrete aggregate, asphalt concrete, fatigue life, freeze-thaw cycles, semicircular bend test**

## 1 Introduction

The volume of construction and demolition waste (CDW) is increasing rapidly, driven by global urbanization and infrastructure development. The effective utilization of CDW has become a critical issue for environmental sustainability. Recycled concrete aggregate (RCA) produced from CDW provides a viable solution for waste management by being beneficially reused in recycled aggregate asphalt concrete (RAAC). However, the mechanical performance and durability of RAAC remain concerns due to the inherent deficiencies of RCA.

RCA exhibits inherent defects such as high porosity, irregular shape and angular texture inherited from the original concrete (Aboutalebi Esfahani, 2020; Zhang et al., 2019). These defects compromise the strength and deformation resistance of RAAC. In particular, the porosity of RCA results in higher water absorption and susceptibility to moisture damage

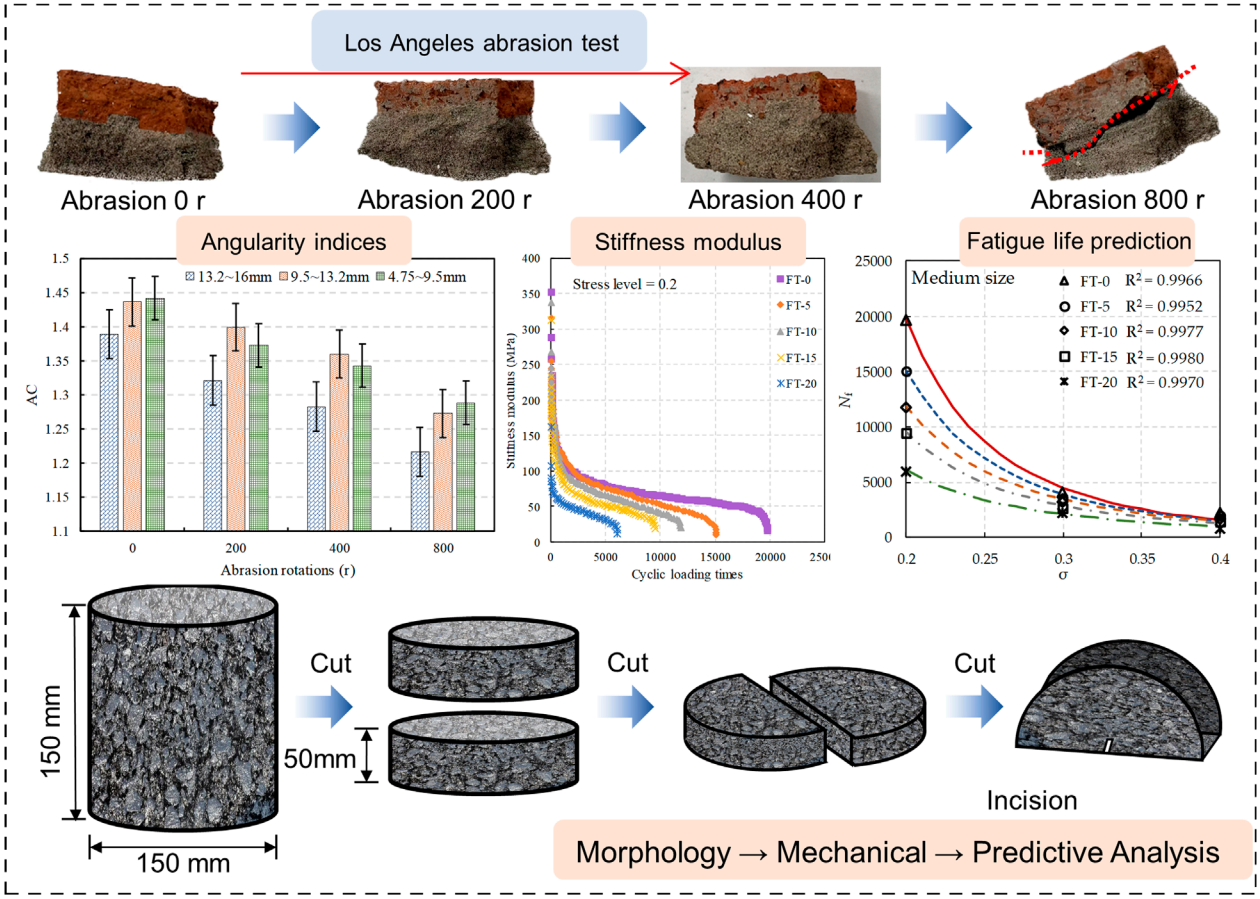


GRAPHICAL ABSTRACT

(Silva et al., 2019; Vieira and Pereira, 2015). Additionally, microcracks formed at the asphalt-aggregate interface during the service life of RAAC weaken its resistance to cracking and fatigue failure under repetitive traffic and environmental loads (Wang R. et al., 2020; Zheng et al., 2021). Previous studies have reported reductions in the resilient modulus, fatigue life and resistance to moisture-induced damage of RAAC compared to conventional asphalt concrete (Sahebzamani et al., 2022; Wang B. et al., 2021; Zieliński, 2024). Therefore, improving the mechanical and durability performance of RAAC requires a more detailed understanding of the physical and morphological characteristics of RCA. These attributes critically influence the long-term behavior and structural integrity of the asphalt mixture.

Fatigue failure stands out as a primary factor contributing to asphalt pavement distress, exerting a significant impact on the long-term performance of asphalt pavements (Li N. et al., 2025; Yao and Xu, 2023; Zhao et al., 2025). Subjected to the combined effects of traffic loading and environmental influences, asphalt pavements experience prolonged periods of stress and strain overlap (Liu et al., 2024; Yang et al., 2024; Zhang et al., 2025). This continuous exposure leads to progressive internal damage and deterioration within the asphalt concrete structure, ultimately compromising its overall integrity (Bazoobandi et al., 2023; Sreedhar and Coleri, 2022; Yousefi et al., 2021). Wang S. et al. (2021) investigated the resistance to fatigue of semi-flexible based pavement across varying temperatures and stress levels, with an in-depth analysis of the fatigue cracking mechanisms in the asphalt surface. Another critical issue is the freeze-thaw (F-T) durability of asphalt pavements in cold regions. The composition of RAAC plays a crucial role in determining the performance of asphalt concrete, with a notable discrepancy in the susceptibility of asphalt mixtures containing different recycled aggregates to F-T cycles (Hosseini et al., 2023; Xiao et al., 2023). Notably, the response of coarse and fine recycled aggregates to F-T induced damage in asphalt concrete varies. Yang et al. (2016) conducted experiments to evaluate the impact of F-T cycles on the fracture energy of asphalt mixtures, revealing the damage behavior of recycled asphalt pavement. During F-T cycles, ingress of moisture into the air voids of RAAC generates development and propagation of internal microcracks (Hao et al., 2018; Xia et al., 2024). The repeated expansion and contraction caused by phase changes of water induce damage accumulation and deterioration of the asphalt-aggregate bond (Feng et al., 2010; Kakar et al., 2015). It has been suggested that the higher porosity and heterogeneity of RCA lead to greater F-T susceptibility compared to natural aggregate asphalt concrete (Akbas et al., 2023; Li et al., 2024b; Upshaw and Cai, 2020). However, limited research has systematically evaluated the effects of combined F-T conditioning and fatigue loading representative of field conditions.

The morphological characteristics of aggregates play a crucial role in determining the mechanical properties and stability of asphalt concrete, encompassing factors such as shape, angularity, and surface texture (Arasan et al., 2011; Cui et al., 2018; Wang et al., 2022). Angularity refers to the extent of protrusions on the surface of aggregate particles. Coarse aggregates with pronounced angularity create a dense interlocking structure, enhancing their strength and stability through an increase in the internal friction angle of RAAC (Ding et al., 2017). Aggregate particles with sharp edges facilitate improved surface texture by interlocking, whereas horizontally oriented flat and elongated particles exhibit shallower interlocking depths (Kogbara et al., 2016). Bessa et al. (2015) demonstrated that increased roughness on the aggregate surface enhances particle-to-particle interface bonding within the asphalt mixture, thereby enhancing the fatigue resistance of the asphalt mixture. In the context of coarse aggregates in asphalt concrete, a preference is given to angular and rough shape characteristics to promote stronger mechanical properties (Olard and Perraton, 2010; Radević et al., 2020). The angular nature of aggregates fosters enhanced interlocking among particles, leading to superior mechanical strength (Wang H. et al., 2020). Conversely, flat and elongated aggregates are prone to breakage, weakening the inter-particle bonding and significantly impacting the mechanical properties of asphalt concrete (Gong et al., 2021; Kong et al., 2019). Studies by Liu et al. (2017) evaluated the fatigue resistance of asphalt mixtures with varying coarse aggregate morphologies, revealing that a higher proportion of spherical aggregates and fewer flake-like aggregates effectively mitigated stiffness degradation. These morphological distinctions directly influence the engineering performance of RCA, with the structural and morphological disparities of RCA rendering it more susceptible to breakage under loading conditions compared to natural aggregates (Li et al., 2024a), consequently affecting the fatigue life of RAAC (Li et al., 2023). Although previous studies have investigated the fatigue performance and F-T durability of recycled asphalt mixtures. Nevertheless, existing research predominantly focused on external factors such as moisture, temperature, and loading conditions. Limited attention has been given to the effects of particle wear, size gradation, and F-T cycles on the fatigue behavior of RAAC, particularly in relation to RCA's evolving morphology during service.

This study contributes a novel perspective to the durability assessment of RAAC by integrating the morphological evolution of RCA with the coupled effects of mechanical fatigue and F-T environmental loading. While earlier research has indicated that finer RCA may enhance asphalt mixture performance, the present work moves beyond this general observation by systematically quantifying RCA morphology changes caused by abrasion. More importantly, it establishes a direct relationship between RCA morphological characteristics and the fatigue life of asphalt concrete under F-T conditions. In addition, a fatigue life prediction model that considers both RCA size and F-T effects is proposed. This approach provides a mechanistic understanding of how geometric properties and environmental stressors jointly influence the long-term structural behavior of asphalt pavements. This study considered RCA size and particle morphology to improve fatigue resistance under combined mechanical and F-T environmental loading. The findings of this research offer critical insights to guide the design and application of recycled materials in sustainable pavement engineering.

# 2 Materials and methods

## 2.1 Materials

### 2.1.1 Asphalt binder

A 70# penetration grade asphalt binder was used in this study. The basic performance tests of the asphalt binder were conducted according to JTG E20-2019 "Standard Test Method of Bitumen and Bituminous Mixtures for Highway Engineering". Table 1 summarizes the test results and specification limits of the asphalt binder.

### 2.1.2 Recycled concrete aggregate

The recycled concrete aggregates (RCA) used in this study were obtained from construction and demolition waste (CDW) processed at a construction site in Changsha, China. The production process of RCA involved primary crushing of CDW, secondary crushing and screening to separate aggregate fractions. The recovered aggregates were then cleaned to produce new RCA.

Figure 1 illustrates the RCA production process from CDW. The CDW was first subjected to primary crushing. It was further crushed and screened into different fractions, followed by washing to obtain the final RCA products.

The gradation curve of the produced RCA is shown in Figure 2. The RCA with different particle sizes were designed to replace natural coarse aggregates in asphalt mixtures. The size ranges of the three replacing RCA were 4.75–9.5 mm, 9.5–13.2 mm and 13.2–16 mm, respectively.

Table 2 summarizes the basic physical properties of the RCA, including apparent density, crushing value, water absorption, Los Angeles abrasion loss and needle flake content. All properties met the specification limits.

The apparent density of RCA was relatively low compared to natural aggregates, which was attributed to the high porosity resulting from cement mortar attaching on aggregate surfaces. The crushing value (representing aggregate crushing resistance) exceeded the maximum limit of 30% specified in some regions such as Europe, suggesting the aggregates were susceptible to crushing under repeated loading. The water absorption of RCA was about 5–7 times that of natural aggregates due to the porous cement paste on the aggregate surface. Both the crushing value and water absorption could deteriorate the volumetric and mechanical properties of asphalt mixtures.

The high Los Angeles abrasion loss indicated that the aggregates were vulnerable to fragmentation and polished surfaces when subjected to vehicle traffic and environmental conditions. The needle flake content of below 10% met the specification limit. Overall, the test results showed the need to improve the moisture resistance and fracture resistance of RCA through rational particle size selection and mixing process optimization when incorporated in asphalt mixtures.

TABLE 1 Properties of 70# asphalt binder.

| Test items | Unit | Results | Requirements | Test method |
|---|---|---|---|---|
| 25°C Needle penetration | 0.1 mm | 60.5 | 60–80 | JTG E20 T 0604 |
| Penetration index (PI) | — | −0.64 | — | JTG E20 T 0604 |
| Softening point | °C | 49.0 | ≥44.0 | JTG E20 T 0606 |
| 10°C ductility | cm | 93.0 | ≥25.0 | JTG E20 T 0605 |
| 15°C density | g/cm$^3$ | 1.032 | — | JTG E20 T 0603 |

### 2.1.3 Mix design of RAAC

By replacing the coarse aggregate with RCA in asphalt concrete, the mix proportions for three RCA components were designed using the Marshall mix design method. For each of the three mixtures, the natural coarse aggregate within the specified size range was fully replaced by 100% RCA. The optimal asphalt content was determined through iterative designs to achieve targets of air voids, voids in mineral aggregate (VMA) and voids filled with asphalt (VFA). Compared to conventional asphalt concrete with natural aggregates, higher asphalt content was required in RAAC to compensate for the higher water absorption and surface flaws of RCA. The high absorption resulted in asphalt coating deficiency on RCA surfaces during the mixing and compaction process. Additional asphalt was thus needed to achieve satisfactory mix workability and volumetrics.

As the RCA size increased from fine to coarse particles, the corresponding optimal asphalt content slightly decreased. This was because the larger RCA particles had lower surface area to volume ratio and were less porous compared to the smaller ones, leading to reduced asphalt demand. Specifically, the determined optimal asphalt binder content was 5.2% for the fine RAAC mixture (4.75–9.5 mm), 5.0% for the medium RAAC mixture (9.5–13.2 mm), and 4.8% for the coarse RAAC mixture (13.2–16 mm). However, all three RAAC mixtures met the specified design criteria. Semi-circular bend (SCB) beam specimens with a diameter of 150 mm and thickness of 50 mm were then prepared from the compacted mixtures for fatigue testing.

## 2.2 Test design

### 2.2.1 Los Angeles abrasion test

The Los Angeles abrasion test was conducted to evaluate the change in angularity of RCA from different size fractions under the action of abrasion. RCA of sizes 4.75–9.5 mm, 9.5–13.2 mm, and 13.2–16 mm were subjected to 0, 200, 400, and 800 rotations in the Los Angeles abrasion machine as shown in Figure 3 to generate RCA materials with different levels of angularity.

Figure 4 displays the morphological characteristics of RCA particles from different size fractions after various rotations. Initially at 0 rotations, RCA surfaces were intact with distinct edges and irregular rough textures resulting from the original composite material. With increasing rotations to 200 and 400, surface abrasion occurred as sharp corners gradually smoothed out and particle shapes became more rounded and regular. Significant fragmentation and surface polishing were observed after 800 rotations, exhibiting the transformation of RCA morphology under prolonged abrasional forces.

After abrasion, the RCA materials were sieved to obtain single-sized fractions within the given size ranges for further testing. Convexity, axiality coefficient (AC) and roundness were selected as angularity indices to quantify the changes in RCA morphology. Each test was conducted in triplicate to ensure repeatability. For each condition, the average value was calculated from three replicates, and the corresponding standard deviation was used to represent data variability.

Convexity is an important indicator for evaluating the complexity of the RCA surface, as shown in Equation 1. The convexity value reflects the regularity of the RCA particle shape. The closer the convexity value is to 1, the more elliptical the shape. Higher convexity values indicate a more irregular aggregate particle surface with more protrusions.

$$Convexity = \frac{C_{convex}}{C_{ellipse}} \tag{1}$$

where $C_{convex}$ is the convex perimeter of the RCA, and $C_{ellipse}$ is the equivalent elliptical perimeter of the RCA.

The AC reflects the elongation of aggregate particles, defined as the ratio of the lengths of the major axis to the minor axis of the equivalent ellipse, as shown in Equation 2. A higher AC may indicate poorer workability and higher internal friction in the RCA, thereby affecting the performance of asphalt concrete.

$$AC = \frac{D_{max}}{D_{min}} \tag{2}$$

where $D_{max}$ and $D_{min}$ are the lengths of the major and minor axes of the equivalent ellipse of the aggregate, respectively.

Roundness is a parameter used to measure the degree to which the shape of RCA particles approximates a circle, as shown in Equation 3.

$$Roundness = \frac{4\pi A}{C^2} \tag{3}$$

where $A$ and $C$ are the projected area and perimeter of the aggregate, respectively.

### 2.2.2 Semi-circular bend (SCB) test

The SCB test was performed to evaluate the fatigue resistance of RAAC. Figure 5 illustrates the fabrication of SCB specimens with a diameter of 150 mm and thickness of 50 mm. A Universal Testing Machine (UTM-100) was employed to load

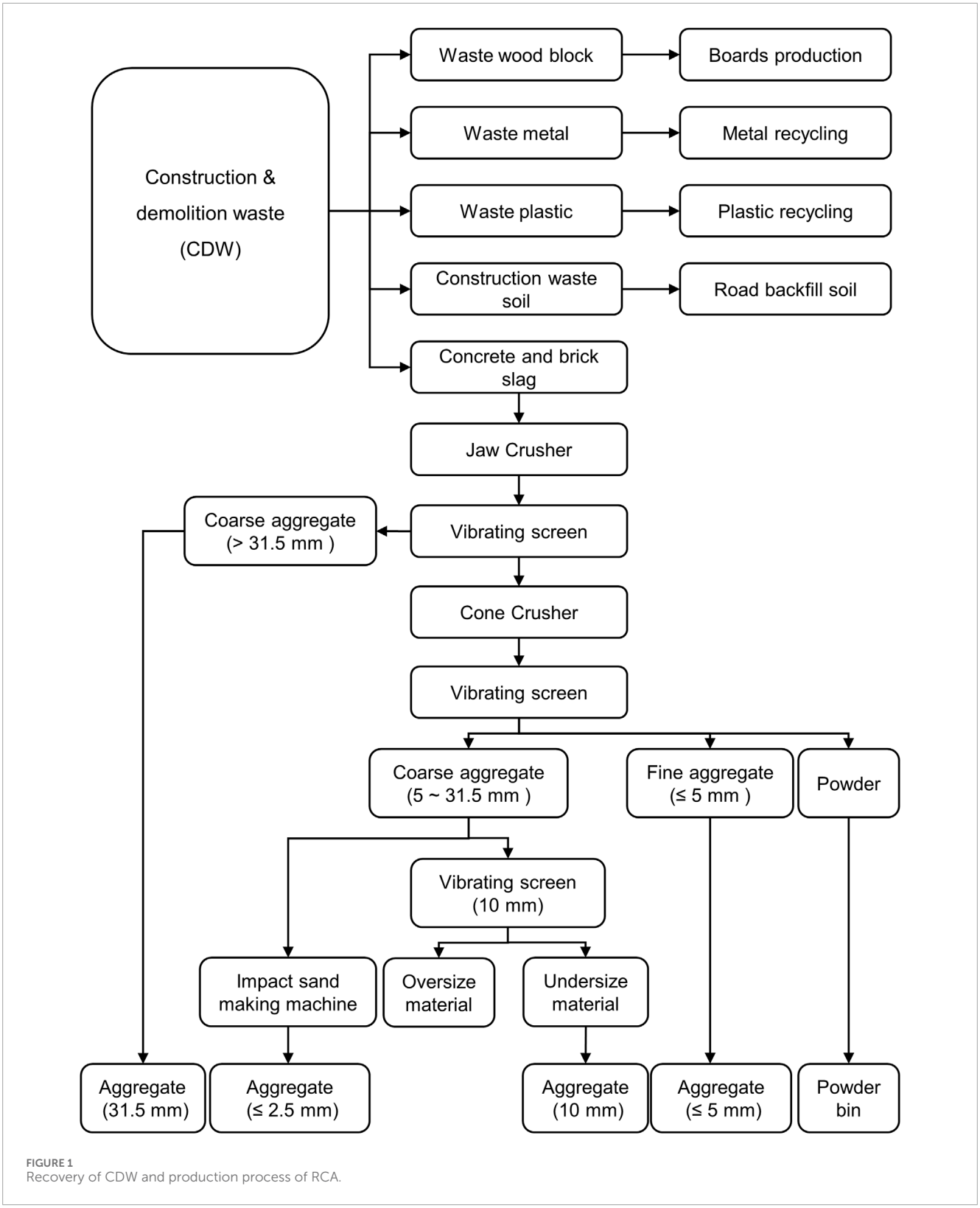


FIGURE 1
Recovery of CDW and production process of RCA.

the SCB specimens in a three-point bending mode with a loading roller diameter of 1 mm and support roller span of 0.8 times the beam diameter.

The stress level, defined as the ratio of applied stress to the maximum tensile stress in the test, is typically employed to simulate the stress state of materials under various loading conditions. In

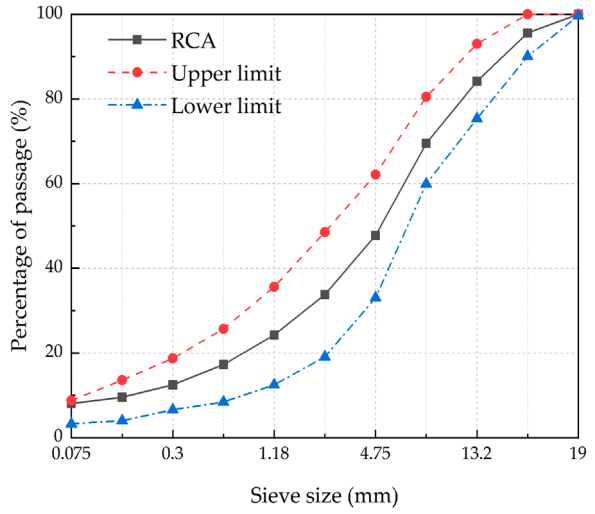


FIGURE 2
The gradation curve of the produced RCA.

cyclic SCB fatigue testing, three loading levels were established based on the maximum tensile stress ($\sigma_t$): 20%, 30%, and 40% of $\sigma_t$, corresponding to distinct stress levels of 0.2, 0.3, and 0.4 respectively. The maximum tensile stress at the bottom of an SCB specimen was determined using Equation 4. In accordance with the recommended specifications outlined in NCHRP 09–46, the loading rate for fracture tests was set at 50 mm/min. The cyclic SCB fatigue tests employed a half-sine wave loading configuration with a period of 0.1 s per cycle. The loading frequency was maintained at 10 Hz, determined based on typical vehicle speeds ranging from 60 to 120 km/h.

$$\sigma_t = \frac{4.976P}{TD} \tag{4}$$

where $P$ is the vertical load, $T$ is the beam thickness and $D$ is the beam diameter.

Stiffness modulus ($S_t$) defined as the slope of the tensile stress-strain curve was used to characterize the damage development in SCB specimens, as shown in Equation 5. Assuming a plane section assumption, the tensile strain ($\varepsilon$) at the beam bottom center was calculated using Equation 6,

$$S_t = \frac{\sigma_t}{\varepsilon} \tag{5}$$

$$\varepsilon = \frac{6Ld}{1.14D^2\left(5.578\frac{L}{d} - 1.3697\right)} \tag{6}$$

where $L$ is the distance between two fixed supports and $d$ is the beam deflection at center.

### 2.2.3 Freeze-thaw test

A F-T test protocol was designed to simulate severe environmental conditioning and accelerate damage accumulation in recycled asphalt concrete. Vacuum-saturated SCB specimens were subjected to freezing at −20°C for 12 h, followed by thawing in a 60°C water bath for 12 h to complete one F-T cycle (JTG E20 2011). The number of cycles applied was 0, 5, 10, 15, and 20 (He and Lu, 2024).

# 3 Results

## 3.1 Effect of abrasion rotations on RCA angularity

The evolution of angularity indices for RCA across various size ranges was quantified as a function of abrasion rotations. As shown in Figure 6a, the initial convexity values around 0.99 reflected the irregularity of RCA particle surfaces across all size fractions. With abrasion, the convexity decreased to around 0.98, suggesting a more uniform distribution of surface asperities due to the porous internal structure of RCA. This transformation is primarily driven by surface polishing, edge chipping, and local fragmentation caused by repeated particle-particle and particle-wall impacts within the Los Angeles abrasion drum. Furthermore, larger RCA particles showed greater fragmentation during abrasion, leading to more pronounced changes in convexity. This is attributed to the higher internal porosity and residual cement mortar in coarse RCA, which make them structurally weaker under impact and frictional forces. Conversely, finer RCA particles generally possess higher surface area-to-volume ratios, facilitating more uniform wear distribution.

It is noteworthy that in Figure 6a, coarse RCA particles exhibit temporary fluctuations in convexity at 200 and 400 revolutions. Convexity is defined as the ratio of the convex perimeter ($C_{convex}$) to the equivalent ellipse perimeter ($C_{ellipse}$), reflecting the boundary irregularity of particles. At intermediate abrasion stages, partial detachment of residual mortar and localized edge fracture may expose new angular features, increasing $C_{convex}$ while $C_{ellipse}$ remains relatively stable. This transient rise or fluctuation in convexity reflects the inherent instability of RCA materials during the abrasion process.

As the rotations number increased to 800, the convexity values tended to stabilize, indicating that RCA particles had reached a relatively stable rounded state. The small RCA size fraction exhibited minimal shape alteration during abrasion, reflected by a limited change in convexity values. The cumulative friction and micro-fracturing removed sharp projections and smoothed the surface features, leading to a reduction in angularity.

In terms of AC (Figure 6b), higher initial values were found for larger RCA sizes suggesting an elongated particle geometry. The AC decreased with increasing rotations as edges smoothed out and shapes became rounder. The reduction was more pronounced for coarse RCA that fragmented and deformed to a larger extent under abrasional forces. This evolution suggests that abrasion not only removes surface asperities but also causes larger structural reshaping, especially in coarse RCA. In contrast, the AC of small RCA remained relatively stable as a result of its integrity against abrasion owing to the finer particle scale. Figure 6c presents the variations of roundness with abrasion rotations. Initially, minor discrepancies in roundness existed among different RCA size ranges. After abrasion treatment, the roundness approached 1, indicating well-rounded particle shapes.

Overall, the abrasion mechanism in RCA is governed by a combination of surface polishing, corner breakage, and internal cracking, especially in porous zones, which reduces angularity and enhances shape regularity. The results confirm that abrasion reduces particle angularity, but angular indices eventually stabilize as

TABLE 2 Basic physical properties of the RCA.

| Items | Tested values | | | Requirements | Specification |
|---|---|---|---|---|---|
| | 4.75–9.5 mm | 9.5–13.2 mm | 13.2–16 mm | | |
| Apparent density (g/cm$^3$) | 2.55 | 2.6 | 2.66 | ≥2.25% | JTG E20 T 0328 |
| Crushing value (%) | 16.9 | 14.8 | 19.2 | ≤30.0% | JTG E20 T 0316 |
| Water absorption (%) | 6.2 | 6.8 | 4.7 | ≤8.0% | JTG E20 T 0307 |
| Los Angeles attrition loss (%) | 24.0 | 24.2 | 27.7 | ≤28.0% | JTG E20 T 0317 |
| Needle flake content (%) | 8.8 | 6.0 | 8.8 | ≤10.0% | JTG E20 T 0312 |

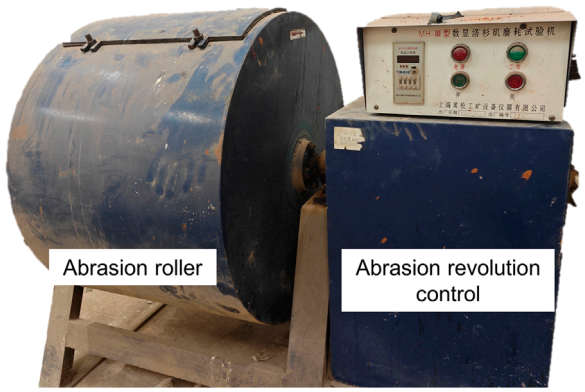


FIGURE 3
Los Angeles abrasion machine.

particles transition to a more equilibrium geometry. In conclusion, fine RCA showed the least shape degradation under abrasion and preserved stable angularity, which is advantageous for asphalt mixture performance. Favorable angularity enhances internal friction and interlocking, ultimately improving structural integrity and load-bearing capacity.

## 3.2 Fatigue life of RAAC with different RCA sizes and F-T cycles

Figure 7 illustrates the fatigue life of RAAC mixtures containing coarse, medium and fine RCA size, subjected to 0, 5, 10, 15 and 20 F-T cycles under stress levels of 0.2, 0.3 and 0.4. The data points in each bar graph represent the mean fatigue life obtained from three replicates, with error bars indicating one standard deviation. The standard deviations were calculated for each test condition to ensure statistical rigor. In general, the fatigue life decreased with increasing F-T cycles regardless of stress level applied.

At a stress level of 0.2 (Figure 7a), F-T cycling significantly affected the fatigue resistance as failures occurred in a linear manner. The internal damages in RAAC propagated and cracks extended more readily when subjected to alternating environmental and mechanical loadings. The phase change of water to ice in pores during freezing generated substantial expansion pressures, severely damaging the aggregate-binder interfaces.

In addition, increment of freeze depth with successive cycles further accumulated ice in pores, worsening the microcracking state. Thawing induced extra pore expansion/contraction and rearranged pore structure, weakening the samples. It was also observed that at a given stress level and F-T condition, different RCA sizes led to distinct fatigue lives. Specifically, the trend was: Coarse size < Medium size < Fine size.

Fine RCA size RAAC mixture exhibited the highest fatigue resistance attributed to its denser microstructure and strong interlocking between filler and coarse aggregates, effectively mitigating the expansion stresses during freezing. Medium RCA size provided moderate particle sizes and structural integrity, while large RCA particles in the coarse mixture lowered the resistance against F-T damages likely due to higher porosity and weaker bonding.

Furthermore, Figure 7 indicates that F-T cycling gradually flattened the slope of S-N curves, especially for coarse RAAC as its sensitivity to stress levels reduced substantially with F-T deterioration. This phenomenon could be explained by the fact that F-T accelerated fatigue damage accumulation so that applied stresses had limited additional effect on the weakened mixtures.

In summary, RCA size and F-T cycles played a vital role in governing the fatigue life of RAAC. Fine RCA size demonstrated optimal resistance against F-T hazards and fatigue failures compared to other sizes.

## 3.3 Stiffness modulus of RAAC under F-T cycles

Figure 8 illustrates the change of RAAC stiffness modulus with the increase of fatigue load cycles under different F-T conditions. Regardless of stress level, RCA size or F-T cycle times, the stiffness modulus steadily decreased as cracking and damage developed within RAAC beams. A three-stage evolution pattern was exhibited, including abrupt change, balance and failure stages.

In the initial stage, fatigue loading rapidly reduced the stiffness due to the formation and propagation of critical cracks. This

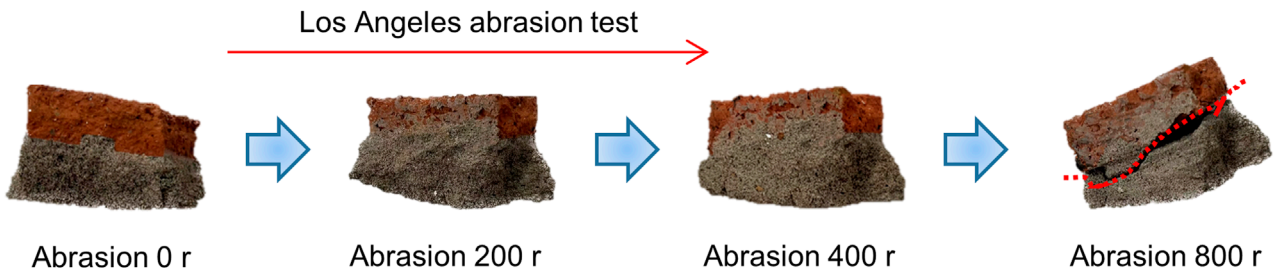


FIGURE 4
The morphological characteristics of RCA particles from different size fractions after various rotations.

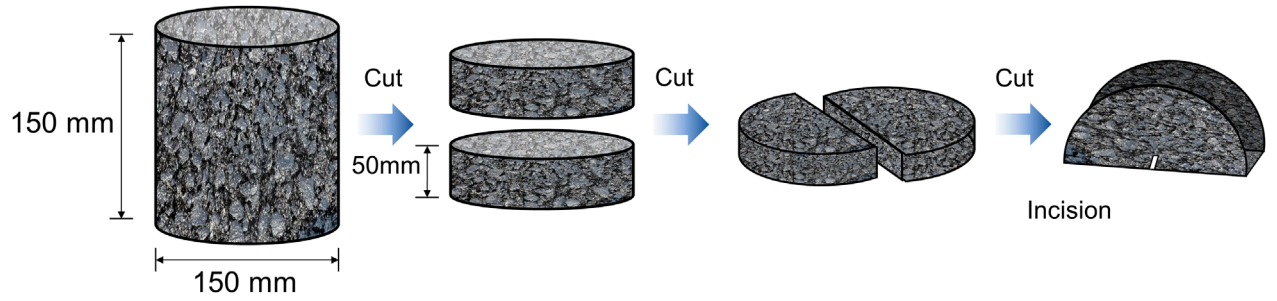


FIGURE 5
The fabrication of SCB specimens.

was attributed to stress concentration at flaws and openings in RAAC. As cracking stabilized through stress redistribution in the samples, the modulus dropped at a steady slow pace during the balance period.

When internal damages accumulated to a critical level, a second sharp decrease occurred until complete failure. As shown in Figure 8a, coarse RCA size mixture presented the most precipitous stiffness loss compared to the medium (Figure 8b) and fine mixtures (Figure 8c). Its higher porosity facilitated moisture ingress and exacerbated expansion stresses during F-T, leading to faster cracking propagation and structural deterioration.

F-T cycles accelerated the reduction of stiffness modulus for all RAAC mixtures. Exposure to alternating freezing and thawing induced cumulative microcrack growth inside the samples by pore pressure effects. Moreover, F-T exacerbated fatigue damage development under cyclic loading, shortening the lifespan before structural instability.

Among the different RCA sizes at equivalent stress levels and F-T conditions, fine RCA size mixture exhibited the highest modulus retention capacity, followed by medium then coarse size. The trend could be attributed to the more compact microstructure and improved interfacial bonding achievable with decreasing particle sizes. In particular, smaller RCA enabled better pore amelioration and reduced damage sensitivity against environmental conditioning.

In summary, RAAC stiffness drastically reduced as a function of both fatigue cycles and F-T exposures. However, rational RCA size for replacement could enhance the resistance of recycled mixtures against coupled fatigue-environmental damages.

# 4 Discussion

## 4.1 Evaluation of angularity indices response to fatigue life

To further assess the relative importance of morphological and environmental parameters on fatigue performance, a gray correlation analysis (GCA) was performed on our test results. The influencing factors include RCA size (coarse, medium and fine), convexity, *AC*, roundness and number of F-T cycles. Fatigue life was considered as a reference sequence. A gray correlation coefficient of more than 0.6 was defined as a strong correlation, while between 0.4 and 0.6 was a moderate correlation. Table 3 summarizes the results of the correlation analysis between the influencing factors and fatigue life.

The correlation results showed that RCA sizes exhibited a strong correlation, and angularity indices and the number of F-T cycles exhibited a moderate correlation. The effect of roundness is the least among them. RCA sizes inherently affect multiple aspects of the asphalt concrete's internal structure, including aggregate packing density, void content, and interfacial bonding area. Finer RCA promotes a denser microstructure and better filler-binder integration, reducing crack initiation points and enhancing fatigue resistance. Conversely, coarse RCA often leads to weaker

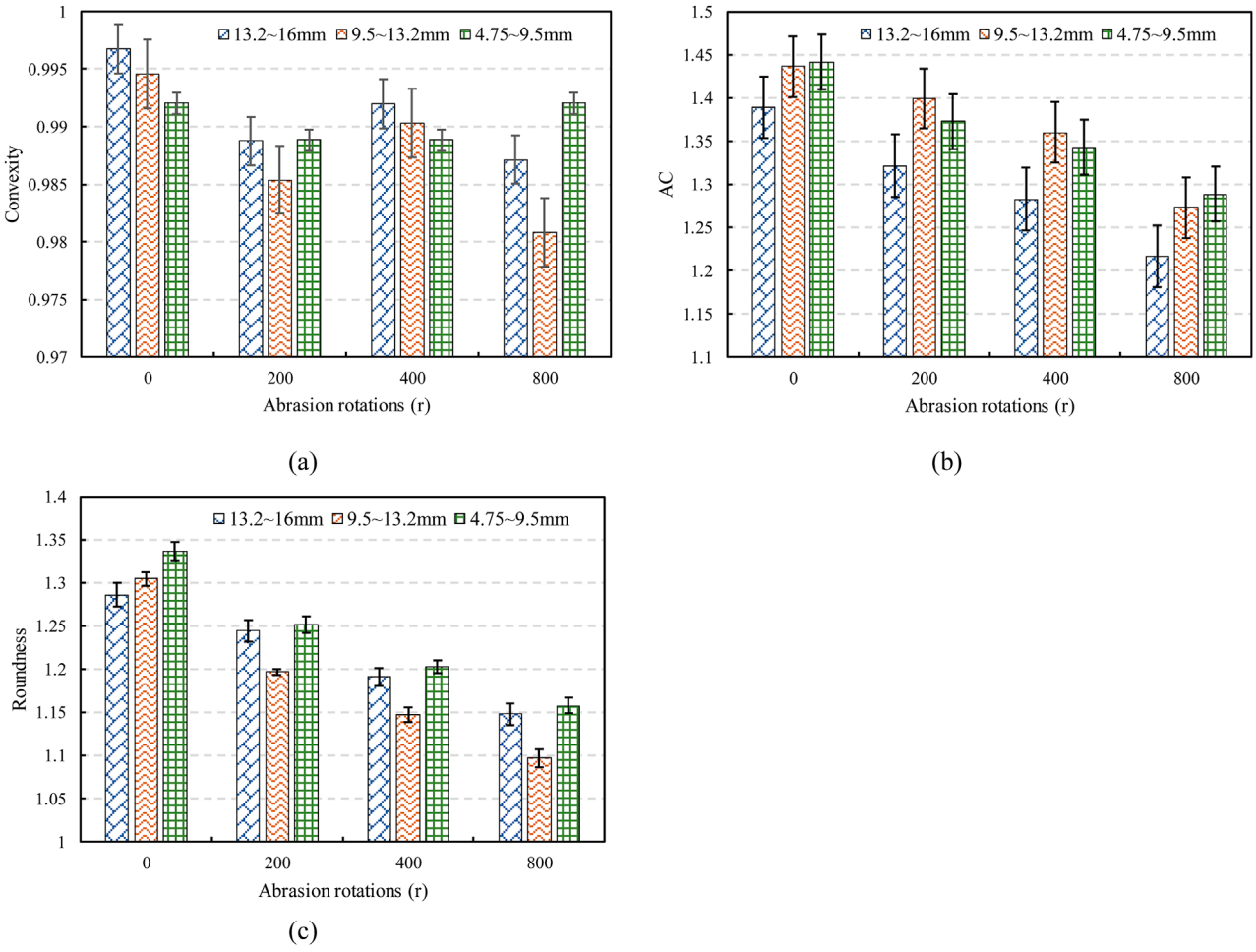


FIGURE 6
The changes in angularity indices of RCA from different size fractions with increasing abrasion rotations: **(a)** Convexity, **(b)** AC and **(c)** Roundness.

interfacial zones and higher porosity, increasing susceptibility to environmental and mechanical deterioration.

Among the three angularity indices, AC demonstrated the highest grey relational grade. This is reasonable because AC reflects particle elongation or anisotropy, which plays a crucial role in load transfer and inter-particle interlock. Elongated particles may enhance frictional contact, limit relative movement, and improve resistance to fatigue crack propagation. Moreover, the beneficial effect of high AC may be more pronounced under F-T cycle damage conditions, where interfacial degradation reduces chemical bonding and mechanical interlock becomes a more dominant factor in maintaining structural integrity.

## 4.2 Fatigue life prediction of RAAC

The fatigue life of RAAC was greatly influenced by RCA size and F-T cycles. Three fatigue life prediction models, namely, the Basquin model, the S-logN model, and the Exponential model, were used for comparative analysis. The results are shown in Table 4 and Figure 9. The Basquin model showed high fitting accuracy under all conditions, with most $R^2$ values exceeding 0.99. This indicates strong predictive performance. Although the S-logN and Exponential models also performed well in some cases, their overall $R^2$ values were lower, especially at early F-T cycles. As the number of F–T cycles increased, the differences among the models became smaller. However, the Basquin model still maintained a clear advantage.

Therefore, the effects of the parameters are discussed further for the Basquin model. Figure 10 shows the fitting curves of fatigue life versus stress level for various RCA size gradations under different F-T conditions, based on the experimental data.

Consistently across gradations, RAAC fatigue life decreased with increasing stress levels, consistent with Basquin's equation. Higher stress levels accelerated crack initiation and propagation, thereby shortening fatigue life. Moreover, F-T cycling contributed to progressive degradation, as evidenced by the general downward shift of fitting curves. Contrary to initial expectations, the fitted Basquin parameter $n$ tended to increase with the number of F-T cycles, indicating that fatigue life became more sensitive to stress levels as the material accumulated microstructural damage. This increasing sensitivity was especially noticeable in coarse RAAC mixture.

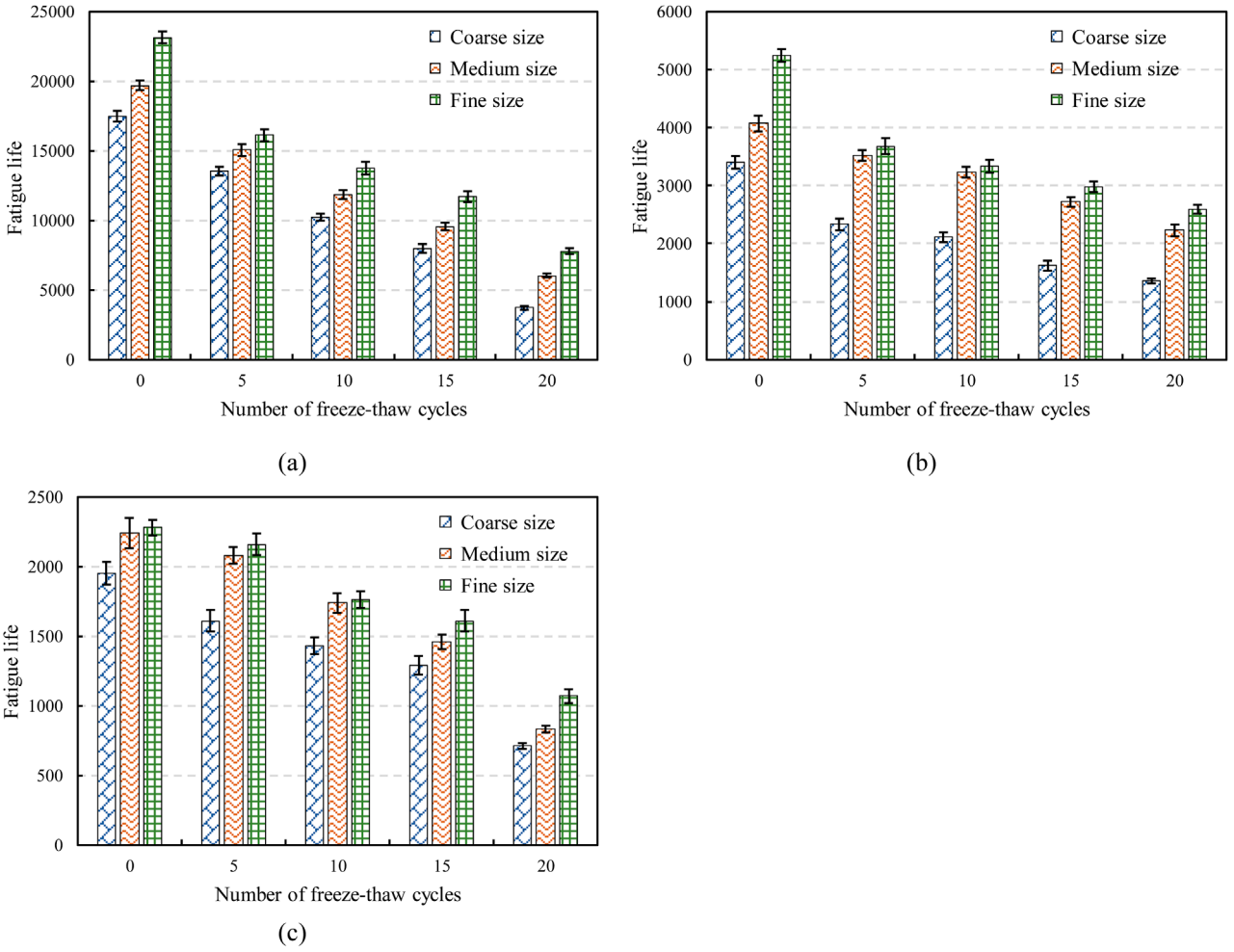


FIGURE 7
The effect of different F-T cycles on the fatigue life of RAAC mixtures with coarse, medium, and fine RCA sizes at stress levels of **(a)** 0.2, **(b)** 0.3, and **(c)** 0.4.

The fatigue parameters $k$ and $n$ were estimated through nonlinear regression and summarized in Table 5, where the associated root mean square error (RMSE) and mean absolute error (MAE) values are also reported to quantify the accuracy of the fitted models. To evaluate the generalization capability of the fatigue life prediction model, both leave-one-out cross-validation (LOOCV) and five-fold cross-validation were performed based on the log–log regression between stress ratio and fatigue life. The average relative prediction error was 4.13% and 4.14%, respectively, indicating high model robustness and predictive reliability across all RCA gradations and F-T conditions.

Parameter $k$ represents the inherent fatigue resistance (higher $k$ values indicate longer fatigue life), whereas $n$ reflects the sensitivity of fatigue life to stress variation (a higher $n$ value signifies stronger stress dependency). As the number of F-T cycles increased, lg$k$ generally decreased, reflecting the material's weakening resistance to repeated loading. Simultaneously, $n$ values increased, demonstrating that stress effects became more dominant in governing fatigue performance under deteriorated conditions. It is evident that both $k$ and $n$ were affected significantly by F-T cycling. For all RCA sizes, the $k$ value generally decreased with increasing F-T cycles from 0 to 20, indicating fatigue resistance reduction. Meanwhile, the $n$ value exhibited an increasing trend, suggesting higher stress responsiveness of RAAC weakened by cyclic environmental damage. This was in line with the flattened S-N curves under more extensive F-T conditioning shown in Figure 9a. Furthermore, at equivalent F-T conditions, fine RCA size mixture achieved the highest k and lowest n amongst the three sizes, inferring its superior resistance against coupled fatigue-environmental effects compared to other sizes. In summary, the fatigue model reasonably characterized the influence of RCA properties and F-T cycles on RAAC durability. Rational size governed the changes of predictive parameters and material performance.

## 4.3 Fracture mechanics perspective on SCB fatigue performance

F-T cycling accelerates fatigue damage in RAAC by promoting early crack development and reducing the mixture's ability to resist

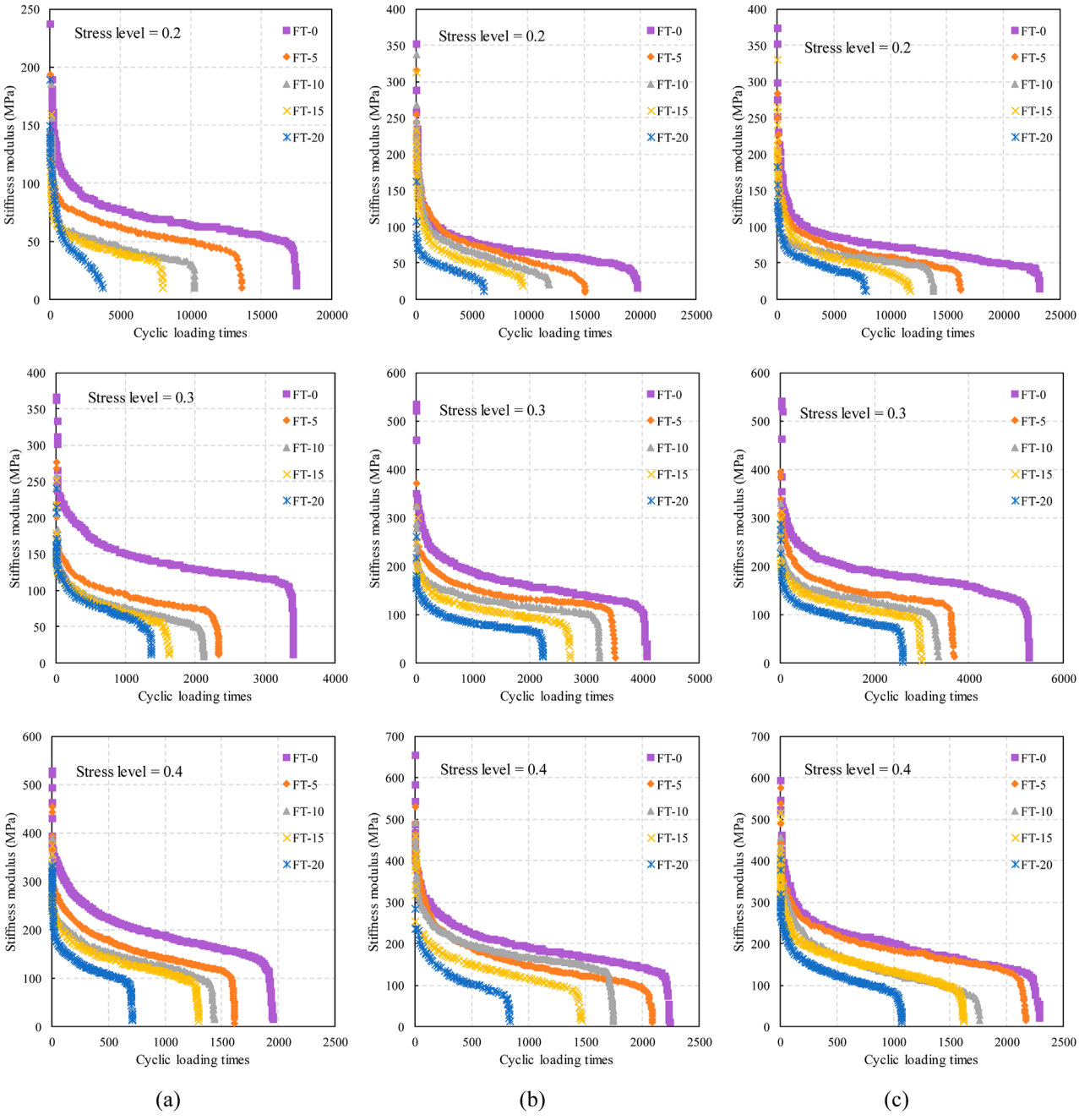


FIGURE 8
Variation of the stiffness modulus of RAAC with coarse **(a)**, medium **(b)**, and fine **(c)** RCA sizes under different F-T cycles as a function of fatigue loading cycles.

fracture. Each F-T cycle introduces micro-cracks and weakens the asphalt–aggregate bond, so less energy is required for a crack to initiate and grow under repeated loading. From a fracture mechanics standpoint, this manifests as a reduction in fracture toughness or fracture energy after conditioning – the material cannot absorb as much strain energy before crack propagation occurs (Launey and Ritchie, 2009). F-T damage causes earlier micro-crack formation, faster macro-crack growth, and premature asphalt–aggregate debonding in asphalt mixtures (Haghighatpour and Aliha, 2023). In terms of energy dissipation, a damaged RAAC specimen will dissipate energy more rapidly through crack extension rather than elastic deformation, which means the critical strain energy release rate is reached in fewer cycles (Li X. et al., 2024). Consequently, the SCB fatigue performance of RAAC drops after F-T exposure because the material's fracture energy threshold has been lowered by internal damage.

The inclusion of recycled concrete aggregates intensifies these fracture effects due to the distinct morphology and interfacial

TABLE 3 Grey correlation analysis results between influence factors and fatigue life.

| Influence factor | Grey correlation coefficient | Degree of correlation |
|---|---|---|
| RCA sizes | 0.604 | Strong correlation |
| Convexity | 0.571 | Moderate correlation |
| AC | 0.574 | Moderate correlation |
| Roundness | 0.526 | Moderate correlation |
| Number of F-T cycles | 0.566 | Moderate correlation |

TABLE 4 Comparison of $R^2$ values for three fatigue life prediction models.

| Number of F-T cycles | RCA sizes | $R^2$ | | |
|---|---|---|---|---|
| | | Basquin | S-logN | Exponential |
| 0 | Coarse | 0.9959 | 0.9679 | 0.9904 |
| | Medium | 0.9966 | 0.9699 | 0.9911 |
| | Fine | 0.9994 | 0.9815 | 0.9962 |
| 5 | Coarse | 0.9922 | 0.9638 | 0.9857 |
| | Medium | 0.9952 | 0.9682 | 0.9876 |
| | Fine | 0.9954 | 0.9683 | 0.9881 |
| 10 | Coarse | 0.9915 | 0.9624 | 0.9829 |
| | Medium | 0.9977 | 0.9759 | 0.9908 |
| | Fine | 0.9976 | 0.9743 | 0.9917 |
| 15 | Coarse | 0.9847 | 0.9560 | 0.9730 |
| | Medium | 0.9980 | 0.9773 | 0.9910 |
| | Fine | 0.9973 | 0.9741 | 0.9907 |
| 20 | Coarse | 0.9998 | 0.9879 | 0.9944 |
| | Medium | 0.9970 | 0.9999 | 0.9999 |
| | Fine | 0.9997 | 0.9960 | 0.9988 |

structure of RCA (Zhang et al., 2023). RCA particles are more porous and often carry residual cement mortar, which creates a weaker interfacial transition zone with the asphalt mastic (Huang et al., 2021; Li M. et al., 2025). Cracks tend to initiate at these flawed interfaces or within the porous RCA itself, rather than through intact binder or strong natural aggregates. This means that less external energy is needed to drive crack growth in RAAC – a significant portion of the fracture process is accommodated by debonding at the RCA mastic interface (Kazemian et al., 2019; Xiao et al., 2022). Recent fracture tests confirm that cracks in RAAC preferentially follow the asphalt-RCA interface, indicating that this is the path of least resistance (Hu et al., 2024). As RCA content increases, the total fracture energy of the mix declines markedly because more crack-prone zones are introduced. In fact, high RCA mixtures (e.g., >50% replacement) exhibit significantly lower SCB fracture resistance, reflecting the dominance of weak RCA interfaces in energy absorption and crack propagation (Hu et al., 2024; Kou et al., 2025). These weaknesses are further exacerbated under F-T conditions. This is mainly due to the fact that water can infiltrate the porous RCA and expand during freezing, widening interfacial transition zone (ITZ) micro-cracks and eroding the asphalt-RCA bond (Ren et al., 2022). The result is a compounding effect in which RAAC after F-T has both a inherently weaker crack-resistant skeleton (due to RCA) and additional micro-fractures from

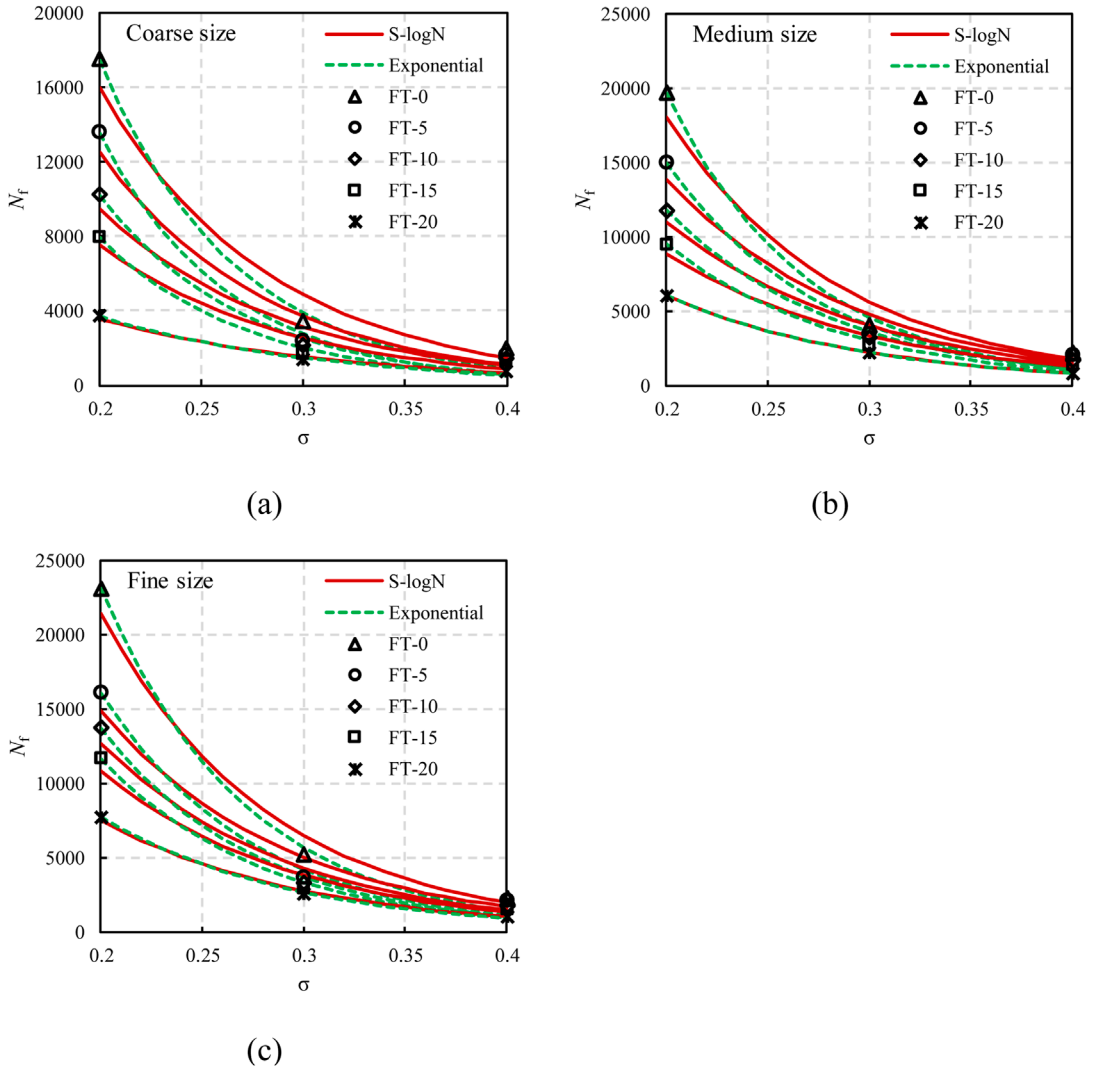


FIGURE 9
Fitted curves of fatigue life and stress level based on S-logN model and exponential model under different F-T cycles: **(a)** coarse size; **(b)** medium size, and **(c)** fine size.

thermal cycling. Thus, when subjected to cyclic bending loads, a F-T damaged RAAC specimen dissipates energy quickly through interfacial cracking and shows accelerated fatigue failure.

In summary, the SCB fatigue life of RAAC is governed by its fracture mechanics–lower fracture toughness in the RCA-modified, F-T leads to easier crack initiation and faster crack growth, explaining the observed reduction in fatigue performance from an energy-based perspective.

## 5 Conclusion

This study investigated the influence of recycled concrete aggregate and freeze-thaw (F-T) cycles on the fatigue performance of recycled asphalt concrete. The following conclusions can be drawn:

(a) Los Angeles abrasion tests revealed that finer RCA fractions underwent less morphological transformation and maintained relatively stable angularity during abrasion. Convexity decreased gradually with increasing abrasion rotations, while axiality coefficient (AC) and roundness stabilized for all RCA size fractions, indicating a balanced morphological evolution.

(b) Semi-circular bend (SCB) tests showed that RCA size and the number of F-T cycles significantly affected RAAC mixtures' fatigue performance. Under equivalent stress levels and environmental conditions, the trend of fatigue followed the order of coarse size replacement < medium size replacement < fine size replacement.

(c) F-T cycling accelerated damage accumulation in RAAC, demonstrated by reductions in fatigue life and stiffness modulus with increasing cycle numbers. Mixtures incorporating fine RCA exhibited the greatest resistance to F-T-induced deterioration, followed by medium and coarse RCA mixtures, respectively. Grey correlation analysis further indicated a strong correlation between RCA size and

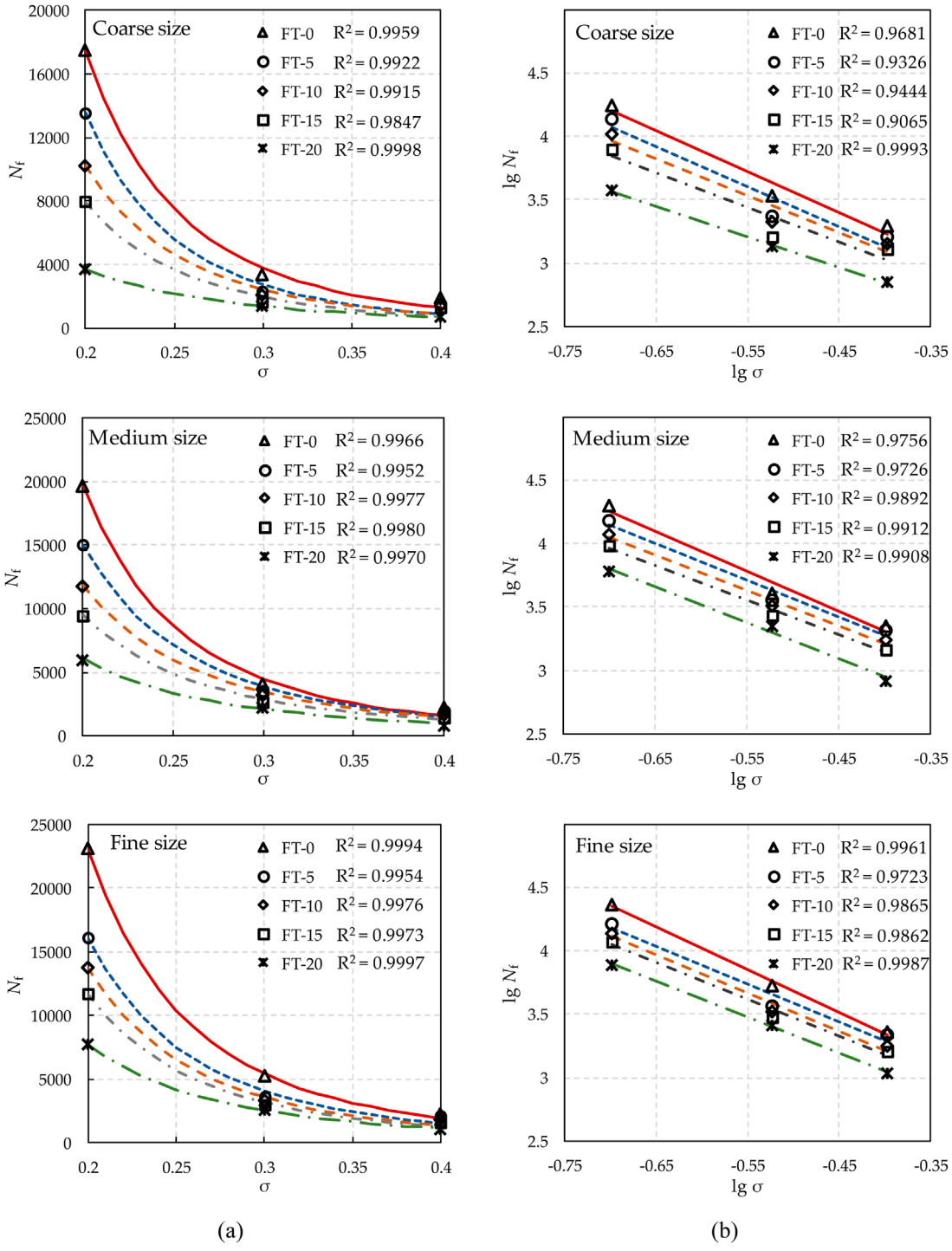


FIGURE 10
Fitted curves of fatigue life and stress levels for mixtures with different RCA sizes under different F-T cycles: **(a)** nonlinear curves; **(b)** linear curves.

fatigue life, while the AC exhibited a moderate correlation, being the more influential morphological index among those analyzed.

(d) A three-stage evolution pattern of stiffness change with fatigue loading comprised an initial abrupt drop, subsequent balanced decline and final failure phase. The presence of F-T cycles significantly exacerbated stiffness degradation. Rational RCA size effectively improved resistance against F-T impacts and retarded structural deterioration.

(e) The fatigue model reasonably predicted the performance through fitting parameters ($R^2 > 0.90$). Both $k$ and $n$ were sensitive to F-T conditioning, while fine size

TABLE 5 Fitted parameters and evaluation metrics for the fatigue life prediction model.

| Number of F-T cycles | RCA sizes | The fatigue parameters | | $R^2$ | RMSE | MAE |
|---|---|---|---|---|---|---|
| | | Lg *k* | *n* | | | |
| 0 | Coarse | 1.949 | 2.395 | 0.9681 | 0.0722 | 0.0677 |
| | Medium | 2.113 | 2.732 | 0.9756 | 0.0622 | 0.0583 |
| | Fine | 2.110 | 2.850 | 0.9961 | 0.0260 | 0.2044 |
| 5 | Coarse | 1.943 | 2.711 | 0.9326 | 0.1048 | 0.0983 |
| | Medium | 2.099 | 2.793 | 0.9726 | 0.0602 | 0.0565 |
| | Fine | 2.021 | 2.894 | 0.9723 | 0.0616 | 0.0578 |
| 10 | Coarse | 1.926 | 2.909 | 0.9444 | 0.0872 | 0.0818 |
| | Medium | 2.051 | 2.834 | 0.9892 | 0.0360 | 0.0337 |
| | Fine | 2.015 | 2.950 | 0.9865 | 0.0434 | 0.0407 |
| 15 | Coarse | 1.892 | 3.156 | 0.9065 | 0.1075 | 0.1009 |
| | Medium | 2.031 | 2.904 | 0.9912 | 0.0319 | 0.0299 |
| | Fine | 1.998 | 3.001 | 0.9862 | 0.0422 | 0.0396 |
| 20 | Coarse | 1.865 | 3.222 | 0.9993 | 0.0076 | 0.0072 |
| | Medium | 1.819 | 3.186 | 0.9908 | 0.0337 | 0.0316 |
| | Fine | 1.905 | 3.365 | 0.9987 | 0.0125 | 0.0117 |

RCA mixture achieved the highest *k* and lowest *n*, suggesting optimal fatigue-environmental resistance amongst the sizes.

In summary, this study established that RCA size selection and F-T cycling significantly influence RAAC fatigue performance. Optimal RCA morphological properties can enhance RAAC durability under combined environmental and mechanical stresses. These findings provide critical insights and guidance for the design and structural evaluation of sustainable asphalt mixtures containing recycled aggregates.

## Data availability statement

The original contributions presented in the study are included in the article/supplementary material, further inquiries can be directed to the corresponding author.

## Author contributions

YY: Software, Writing – original draft, Data curation, Formal Analysis, Investigation, Validation. WL: Conceptualization, Supervision, Project administration, Writing – original draft, Investigation, Methodology. LW: Writing – original draft, Methodology, Conceptualization, Investigation, Formal Analysis, Writing – review and editing.

## Funding

The author(s) declare that no financial support was received for the research and/or publication of this article.

## Conflict of interest

The authors declare that the research was conducted in the absence of any commercial or financial relationships that could be construed as a potential conflict of interest.

## Generative AI statement

The author(s) declare that no Generative AI was used in the creation of this manuscript.

## Publisher's note



## References

Aboutalebi Esfahani, M. (2020). Evaluating the feasibility, usability, and strength of recycled construction and demolition waste in base and subbase courses. *Road. Mater. Pavement Des.* 21, 156–178. doi:10.1080/14680629.2018.1483259

Akbas, M., Ozaslan, B., and Iyisan, R. (2023). Utilization of recycled concrete aggregates for developing high-performance and durable flexible pavements. *Constr. Build. Mater.* 407, 133479. doi:10.1016/j.conbuildmat.2023.133479

Arasan, S., Yenera, E., Hattatoglu, F., Hinislioglua, S., and Akbuluta, S. (2011). Correlation between shape of aggregate and mechanical properties of asphalt concrete: digital image processing approach. *Road. Mater. Pavement Des.* 12, 239–262. doi:10.1080/14680629.2011.9695245

Bazoobandi, P., Karimi, H. R., Mousavi, S. R., Karimi, F., and Aliha, M. (2023). Full range of mode I and ii cracking performance of asphalt mixtures containing low to high reclaimed asphalt pavement (rap) contents; modified by recycling agent and substituting of a softer binder. *Case Stud. Constr. Mater.* 19, e02487. doi:10.1016/j.cscm.2023.e02487

Bessa, I. S., Branco, V. T. C., Soares, J. B., and Neto, J. A. N. (2015). Aggregate shape properties and their influence on the behavior of hot-mix asphalt. *J. Mater. Civ. Eng.* 27, 04014212. doi:10.1061/(asce)mt.1943-5533.0001181

Cui, P., Xiao, Y., Yan, B., Li, M., and Wu, S. (2018). Morphological characteristics of aggregates and their influence on the performance of asphalt mixture. *Constr. Build. Mater.* 186, 303–312. doi:10.1016/j.conbuildmat.2018.07.124

Ding, X., Ma, T., and Gao, W. (2017). Morphological characterization and mechanical analysis for coarse aggregate skeleton of asphalt mixture based on discrete-element modeling. *Constr. Build. Mater.* 154, 1048–1061. doi:10.1016/j.conbuildmat.2017.08.008

Feng, D., Yi, J., Wang, D., and Chen, L. (2010). Impact of salt and freeze–thaw cycles on performance of asphalt mixtures in coastal frozen region of China. *Cold Regions Sci. Technol.* 62, 34–41. doi:10.1016/j.coldregions.2010.02.002

Gong, F., Liu, Y., You, Z., and Zhou, X. (2021). Characterization and evaluation of morphological features for aggregate in asphalt mixture: a review. *Constr. Build. Mater.* 273, 121989. doi:10.1016/j.conbuildmat.2020.121989

Haghighatpour, P. J., and Aliha, M. (2023). The influence of recycled asphalt pavement materials on low and intermediate fracture behavior of asphalt concrete (Ac) after exposing to different thawing and freezing periods. *Eng. Fract. Mech.* 293, 109715. doi:10.1016/j.engfracmech.2023.109715

Hao, L., Liu, Y., Wang, W., Zhang, J., and Zhang, Y. (2018). Effect of salty freeze-thaw cycles on durability of thermal insulation concrete with recycled aggregates. *Constr. Build. Mater.* 189, 478–486. doi:10.1016/j.conbuildmat.2018.09.033

He, R., and Lu, N. (2024). Hydration, fresh, mechanical, and freeze-thaw properties of cement mortar incorporated with polymeric microspheres. *Adv. Compos. Hybrid Mater.* 7, 92. doi:10.1007/s42114-024-00899-2

Hosseini, S. G., Kordani, A. A., and Zarei, M. (2023). Effect of recycled additives on pure mode I fracture resistance and moisture susceptibility of hot mix asphalt (hma): an experimental study using semicircular bending (scb) and indirect tensile strength (its) tests. *Theor. Appl. Fract. Mech.* 128, 104168. doi:10.1016/j.tafmec.2023.104168

Hu, J., Zhao, W., Liu, P., Huang, Q., and Luo, S. (2024). Study on fracture characteristics of recycled aggregates asphalt concrete. *Constr. Build. Mater.* 419, 135431. doi:10.1016/j.conbuildmat.2024.135431

Huang, Q., Qian, Z., Hu, J., Zheng, D., Chen, L., Zhang, M., et al. (2021). Investigation on the properties of aggregate-mastic interfacial transition zones (itzs) in asphalt mixture containing recycled concrete aggregate. *Constr. Build. Mater.* 269, 121257. doi:10.1016/j.conbuildmat.2020.121257

JTG E20 (2011). *Standard test methods of bitumen and bituminous mixtures for Highway engineering*. Beijing, China: JTG E20; Ministry of Transport of the People's Republic of China.

Kakar, M. R., Hamzah, M. O., and Valentin, J. (2015). A review on moisture damages of hot and warm mix asphalt and related investigations. *J. Clean. Prod.* 99, 39–58. doi:10.1016/j.jclepro.2015.03.028

Kazemian, F., Rooholamini, H., and Hassani, A. (2019). Mechanical and fracture properties of concrete containing treated and untreated recycled concrete aggregates. *Constr. Build. Mater.* 209, 690–700. doi:10.1016/j.conbuildmat.2019.03.179

Kogbara, R. B., Masad, E. A., Kassem, E., Scarpas, A. T., and Anupam, K. (2016). A state-of-the-art review of parameters influencing measurement and modeling of skid resistance of asphalt pavements. *Constr. Build. Mater.* 114, 602–617. doi:10.1016/j.conbuildmat.2016.04.002

Kong, D., Chen, M., Xie, J., Zhao, M., and Yang, C. (2019). Geometric characteristics of bof slag coarse aggregate and its influence on asphalt concrete. *Materials* 12, 741. doi:10.3390/ma12050741

Kou, C., Fan, R., Zhang, M., Zhu, Z., Kang, A., and Baaj, H. (2025). Investigation into the crack propagation behaviors of asphalt mixture containing recycled concrete aggregates using digital image correlation. *Constr. Build. Mater.* 470, 140636. doi:10.1016/j.conbuildmat.2025.140636

Launey, M. E., and Ritchie, R. O. (2009). On the fracture toughness of advanced materials. *Adv. Mater.* 21, 2103–2110. doi:10.1002/adma.200803322

Li, J., Qin, Y., Zhang, J., Zhang, A., and Zhang, X. (2024a). Compaction and shear characteristics of recycled construction and demolition aggregates in subgrade: exploring particle breakage and shape effects. *J. Clean. Prod.*, 142776. doi:10.1016/j.jclepro.2024.142776

Li, J., Qin, Y., Zhang, X., Shan, B., and Liu, C. (2024b). Emission characteristics, environmental impacts, and health risks of volatile organic compounds from asphalt materials: a state-of-the-art review. *Energy and Fuels* 38, 4787–4802. doi:10.1021/acs.energyfuels.3c04438

Li, J., Zhang, J., Yang, X., Zhang, A., and Yu, M. (2023). Monte Carlo simulations of deformation behaviour of unbound granular materials based on a real aggregate library. *Int. J. Pavement Eng.* 24, 2165650. doi:10.1080/10298436.2023.2165650

Li M., M., Xie, J., Zhang, L., Wu, S., Li, C., Sun, Q., et al. (2025). Investigation of a novel method to improve the physical properties of recycled concrete aggregate for asphalt mixtures: laboratory characterization and mechanisms. *J. Mater. Civ. Eng.* 37, 04025074. doi:10.1061/jmcee7.mteng-19114

Li N., N., Morozov, I. B., Fu, L. Y., and Deng, W. (2025). Unified nonlinear elasto-visco-plastic rheology for bituminous rocks at variable pressure and temperature. *J. Geophys. Res. Solid Earth* 130, e2024JB029295. doi:10.1029/2024jb029295

Li, X., An, H., Chen, Y., Qin, Y., Li, Y., and Zhou, Y. (2024). Mechanical properties of recycled aggregate concrete under cyclic loading and unloading in alpine areas. *J. Build. Eng.* 85, 108759. doi:10.1016/j.jobe.2024.108759

Liu, X., Liu, X., Zhang, Z., and Ai, X. (2024). Effect of carbonation curing on the characterization and properties of steel slag-based cementitious materials. *Cem. Concr. Compos.* 154, 105769. doi:10.1016/j.cemconcomp.2024.105769

Liu, Y., Huang, Y., Sun, W., Nair, H., Lane, D. S., and Wang, L. (2017). Effect of coarse aggregate morphology on the mechanical properties of stone matrix asphalt. *Constr. Build. Mater.* 152, 48–56. doi:10.1016/j.conbuildmat.2017.06.062

Olard, F., and Perraton, D. (2010). On the optimization of the aggregate packing characteristics for the design of high-performance asphalt concretes. *Road. Mater. Pavement Des.* 11, 145–169. doi:10.1080/14680629.2010.9690330

Radević, A., Isailović, I., Wistuba, M. P., Zakić, D., Orešković, M., and Mladenović, G. (2020). The impact of recycled concrete aggregate on the stiffness, fatigue, and low-temperature performance of asphalt mixtures for road construction. *Sustainability* 12, 3949. doi:10.3390/su12103949

Ren, H., Qian, Z., Lin, B., Huang, Q., Crispino, M., and Ketabdari, M. (2022). Effect of recycled concrete aggregate features on adhesion properties of asphalt mortar-aggregate interface. *Constr. Build. Mater.* 353, 129097. doi:10.1016/j.conbuildmat.2022.129097

Sahebzamani, H., Alavi, M. Z., Farzaneh, O., and Moniri, A. (2022). Laboratory and field investigation of the effect of polymerized pellets on the fatigue and low-temperature performance of asphalt mixtures. *Constr. Build. Mater.* 323, 126527. doi:10.1016/j.conbuildmat.2022.126527

Silva, R., De Brito, J., and Dhir, R. (2019). Use of recycled aggregates arising from construction and demolition waste in new construction applications. *J. Clean. Prod.* 236, 117629. doi:10.1016/j.jclepro.2019.117629

Sreedhar, S., and Coleri, E. (2022). The effect of long-term aging on fatigue cracking resistance of asphalt mixtures. *Int. J. Pavement Eng.* 23, 308–320. doi:10.1080/10298436.2020.1745206

Upshaw, M., and Cai, C. (2020). Critical review of recycled aggregate concrete properties, improvements, and numerical models. *J. Mater. Civ. Eng.* 32, 03120005. doi:10.1061/(asce)mt.1943-5533.0003394

Vieira, C. S., and Pereira, P. M. (2015). Use of recycled construction and demolition materials in geotechnical applications: a review. *Resour. Conserv. Recycl.* 103, 192–204. doi:10.1016/j.resconrec.2015.07.023

Wang, B., Yan, L., Fu, Q., and Kasal, B. (2021). A comprehensive review on recycled aggregate and recycled aggregate concrete. *Resour. Conserv. Recycl.* 171, 105565. doi:10.1016/j.resconrec.2021.105565

Wang, H., Wang, C., Bu, Y., You, Z., Yang, X., and Oeser, M. (2020). Correlate aggregate angularity characteristics to the skid resistance of asphalt pavement based on image analysis Technology. *Constr. Build. Mater.* 242, 118150. doi:10.1016/j.conbuildmat.2020.118150

Wang, L., Yao, Y., Li, J., Tao, Y., and Liu, K. (2022). Review of visualization technique and its application of road aggregates based on morphological features. *Appl. Sci.* 12, 10571. doi:10.3390/app122010571

Wang, R., Yu, N., and Li, Y. (2020). Methods for improving the microstructure of recycled concrete aggregate: a review. *Constr. Build. Mater.* 242, 118164. doi:10.1016/j.conbuildmat.2020.118164

Wang, S., Zhou, H., Chen, X., Gong, M., Hong, J., and Shi, X. (2021). Fatigue resistance and cracking mechanism of semi-flexible pavement mixture. *Materials* 14, 5277. doi:10.3390/ma14185277

Xia, P., Khan, S., Tahir, M., Hassam, M., Gong, F., and Zhao, Y. (2024). Characterizations and quantification of freeze-thaw behaviors of recycled brick aggregate concrete. *J. Build. Eng.* 86, 108821. doi:10.1016/j.jobe.2024.108821

Xiao, J., Tang, Y., Chen, H., Zhang, H., and Xia, B. (2022). Effects of recycled aggregate combinations and recycled powder contents on fracture behavior of fully recycled aggregate concrete. *J. Clean. Prod.* 366, 132895. doi:10.1016/j.jclepro.2022.132895

Xiao, X., Li, J., Cai, D., Lou, L., Shi, Y., and Xiao, F. (2023). Low-temperature cracking resistance of asphalt concretes for railway substructure exposed to repeated freeze-thaw cycles. *Cold Regions Sci. Technol.* 206, 103721. doi:10.1016/j.coldregions.2022.103721

Yang, L., Gao, Y., Chen, H., Jiao, H., Dong, M., Bier, T. A., et al. (2024). Three-dimensional concrete printing Technology from a rheology perspective: a review. *Adv. Cem. Res.* 36, 567–586. doi:10.1680/jadcr.23.00205

Yang, S., Braham, A., Wang, L., and Wang, Q. (2016). Influence of aging and moisture on laboratory performance of asphalt concrete. *Constr. Build. Mater.* 115, 527–535. doi:10.1016/j.conbuildmat.2016.04.063

Yao, X., and Xu, T. (2023). Fatigue fracture and self-healing behaviors of cold recycled emulsified asphalt mixture containing microcapsules based on semicircular bending test. *J. Clean. Prod.* 410, 137171. doi:10.1016/j.jclepro.2023.137171

Yousefi, A. A., Sobhi, S., Aliha, M. M., Pirmohammad, S., and Haghshenas, H. (2021). Cracking properties of warm mix asphalts containing reclaimed asphalt pavement and recycling agents under different loading modes. *Constr. Build. Mater.* 300, 124130. doi:10.1016/j.conbuildmat.2021.124130

Zhang, H., Liu, H., Deng, Y., Cao, Y., He, Y., Liu, Y., et al. (2025). Fatigue behavior of high-strength steel wires considering coupled effect of multiple corrosion-pitting. *Corros. Sci.* 244, 112633. doi:10.1016/j.corsci.2024.112633

Zhang, L., Sojobi, A., Kodur, V., and Liew, K. (2019). Effective utilization and recycling of mixed recycled aggregates for a greener environment. *J. Clean. Prod.* 236, 117600. doi:10.1016/j.jclepro.2019.07.075

Zhang, T., Chen, M., Wang, Y., and Zhang, M. (2023). Roles of carbonated recycled fines and aggregates in hydration, microstructure and mechanical properties of concrete: a critical review. *Cem. Concr. Compos.* 138, 104994. doi:10.1016/j.cemconcomp.2023.104994

Zhao, Y., Lu, Z., Gedela, R., Tang, C., Feng, Y., Liu, J., et al. (2025). Performance and geocell-soil interaction of sand subgrade reinforced with high-density polyethylene, polyester, and polymer-blend geocells: 3d numerical studies. *Comput. Geotechnics* 178, 106949. doi:10.1016/j.compgeo.2024.106949

Zheng, Y., Zhang, Y., and Zhang, P. (2021). Methods for improving the durability of recycled aggregate concrete: a review. *J. Mater. Res. Technol.* 15, 6367–6386. doi:10.1016/j.jmrt.2021.11.085

Zieliński, P. (2024). The use of the semi-circular bending method to assess the intermediate-temperature fracture toughness of asphalt concrete mixes with reclaimed asphalt shingles. *Road. Mater. Pavement Des.* 25, 81–98. doi:10.1080/14680629.2023.2194432